MAXIMUM RUN-UP BEHAVIOR OF TSUNAMIS UNDER NON-ZERO INITIAL VELOCITY CONDITION

Baran AYDIN [*]

Department of Civil Engineering, Faculty of Engineering, Adana Science and Technology University, Adana, Turkey

ABSTRACT

The tsunami run-up problem is solved non-linearly under the most general initial conditions, that is, for realistic initial waveforms such as N-waves, as well as standard initial waveforms such as solitary waves, in the presence of initial velocity. An initial-boundary value problem governed by the non-linear shallow-water wave equations is solved analytically utilizing the classical separation of variables technique, which proved to be not only fast but also accurate analytical approach for this type of problems. The results provide important information on maximum tsunami run-up qualitatively. We observed that, although the calculated maximum run-ups increase significantly, going as high as double that of the zero-velocity case, initial waves having non-zero fluid velocity exhibit the same run-up behavior as waves without initial velocity, for all wave types considered in this study.

Keywords: Tsunami, Run-up, Non-zero initial velocity, Analytical solution

1. INTRODUCTION

Tsunami is a Japanese word, meaning harbor ("tsu") wave ("nami"), entered in almost all languages, especially after the great 26 December 2004 Indian Ocean tsunami, and used to refer a series of sea surface waves resulting from sudden disturbance of the seafloor, mostly an underwater earthquake (75%) or landslide (10%) [1]. The time between subsequent wave crests during a tsunami can vary from minutes to an hour, while the waves may be persistent for many hours after the displacement of the seafloor. Impact of a tsunami can vary significantly from one part of the coast to the other because of factors like features of local bathymetry and the shape and elevation of the shoreline [2]. The wave height measured at any point of interest on the shoreline is defined to be *tsunami run-up* at that point. Run-up is a function of time, and its maximum over the entire time is called the *maximum run-up*. Accurate calculation of the maximum tsunami run-up is extremely crucial since it is one of the main inputs, together with inundation distance, both for pre-disaster risk reduction efforts and for post-disaster management.

Calculating maximum run-up has always been a difficult task as it depends on many factors such as the character of the initial wave, features of the seafloor, and even the state of the tide at the time the waves reach the shore. The common approach to simplify this task and to estimate the maximum run-up height is the *plane beach* assumption. This approach assumes linearly sloping sea bottom and is convenient for both theoretical and experimental studies. The advantage of this assumption from theoretical point of view is simplification of the differential equations that govern the wave propagation, while the usefulness for experimental studies is ease in constructing a wave flume with linear slope. Resulting theoretical or empirical equations which relate maximum run-up of tsunamis to certain geometrical parameters such as initial wave amplitude and beach slope are known as *run-up laws*.

Run-up laws in the literature have mostly been derived for solitary waves. This is because this family of waves had been used as the standard initial condition for tsunamis until 1990s. The extensive literature

on the propagation and run-up of solitary waves includes analytical [3-6,14], numerical [7-11], and experimental [12-14] studies. To mention several landmark studies in details, Hall & Watts [12] studied propagation of non-breaking solitary waves in laboratory conditions and they were the first to derive an empirical run-up law for such waves relating the maximum run-up to the initial wave amplitude and beach slope. Synolakis [6] derived the run-up law of solitary waves analytically and verified his results with experimental data. In his pioneering study [6] also proved the *run-up invariance* for solitary waves: the maximum run-up predicted by the linear shallow-water wave theory is exactly the same as the one that is predicted by the non-linear theory. His study has been used as a benchmark for most of the later studies, either analytical or numerical, as stated by [15], to whom the reader is referred to for a much comprehensive history of tsunami hydrodynamics.

In 1994, Tadepalli & Synolakis [16] offered a family of depression-elevation waves, called N-waves (since their cross-sections look like the letter "N") as more realistic initial condition for tsunamis. Indeed, N-waves better simulate, compared to solitary waves, the first receding and then rising sea state during a tsunami. [16] also derived analytical run-up laws for N-waves.

The run-up laws for either solitary or N-waves are derived under the acceptance that the spatial distribution of the initial fluid velocity is identically zero. This approach assumes that earthquake rupture speed is much greater than the speed of water in the vertical direction. The practice in the case of earthquake-generated tsunamis is then translating the sea bottom fault displacement directly to the free surface to establish tsunami initial wave. However, the time scale of the generation mechanism should be accounted if the tsunami is triggered by a slowly rupturing earthquake or a submarine landslide. The initial fluid velocity has a non-zero spatial distribution in this case and it plays an important role in the subsequent wave propagation. Kanoglu & Synolakis [17] derived such solution for the shallow-water wave equations and obtained non-linear evolution and run-up of different combinations of the Gaussian (bell-shaped) initial wave.

This study compares the run-up behavior of solitary and N-wave type initial profiles, having zero and non-zero initial velocities. We will resolve the wave field by using an analytical model governed by the non-linear shallow-water wave equations. We will then calculate the maximum run-up of solitary waves and N-waves in the presence of initial velocity and compare with results for the zero-velocity case. We will also change certain geometrical parameters of the initial waves to observe how these parameters affect the maximum run-up.

2. MATHEMATICAL ANALYSIS

2.1. Formulation of the Initial-boundary Value Problem

Although there are a variety of analytical models in the tsunami literature, the standard equations used for run-up calculations are the shallow-water wave equations. Like all equations modeling fluid flow, they are derived from the combination of the Navier-Stokes and the continuity equations under certain assumptions, the details of which can be found in classical texts [5,18]. Below we present the initial-boundary value problem formulated by [19]. Expressed in non-dimensional quantities, the governing equations are the non-linear shallow-water equations, i.e.

$$\eta_t + [(x + \eta) u]_x = 0, \ u_t + u u_x + \eta_x = 0, \tag{1a,b}$$

subject to the boundary conditions

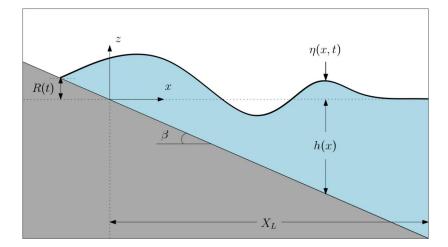$$|\eta(x = 0, t)| < \infty, \qquad \eta(x = X_L, t) = 0, \tag{2a,b}$$

Figure 1. Definition sketch (not to scale). Note that in $h(x) = x$ in non-dimensional form

and to the initial conditions

$$\eta(x, t = 0) = \eta_0(x), \quad u(x, t = 0) = u_0(x). \tag{3a,b}$$

Equations (1) are to be solved for the free surface elevation $\eta(x, t)$ and the horizontal fluid velocity $u(x, t)$. The subscripts denote partial derivatives. $X_S \leq x \leq X_L$ and $0 \leq t$ are the space and the time variables, respectively, where $X_S(t)$ is the instantaneous shoreline tip, with $X_S(0) = 0$ (i.e. the initial shoreline is at $x = 0$), and X_L is the open sea boundary (Figure 1). Equations (2) define the boundary data. The first condition requires the wave height to have a finite value at the initial shoreline for a physical solution. The second condition requires the open boundary to be far offshore. We could also impose $u(x = X_L, t) = 0$ at this boundary, which would lead the same shoreline variation and run-up for any given initial wave profile [20]. Equations (3) describe the initial sea state, that is, the spatial distribution of the initial surface profile and the associated initial velocity. In the model used in this study, both $\eta_0(x)$ and $u_0(x)$ are assumed to be non-zero in order to obtain the most general solution.

2.1. Solution Through Eigenfunction Expansion

The initial-boundary value problem defined in equations (1)-(3) can be solved with different methods. Majority of the solutions in the literature use integral transform methods. However, such solutions have several drawbacks, as explained in [19], who suggested a more convenient solution through the separation of variables method. With this method propagation and run-up of a variety of initial waveforms with and without initial velocity can be calculated easily and accurately.

[19] first uses the *hodograph transformation* ($\sigma^2 = x + \eta$, $\lambda = t - u$) introduced by Carrier & Greenspan [3], to convert the system in equations (1) of two first-order non-linear coupled differential equations into a single second-order linear equation, $4\sigma\varphi_{\lambda\lambda} - (\sigma\varphi_\sigma)_\sigma = 0$, where $\varphi = \eta + u^2/2$, sometimes called the *potential function*. So, the new independent variables of the problem are now σ and λ, replacing x and t, respectively. Besides, with this transformation, the moving shoreline tip $X_S(t)$ in the physical coordinates is fixed to the point $\sigma = 0$ in the new coordinates, through which the difficulty in calculating temporal variation of the moving shoreline can be avoided. Moreover, unlike equations (1), the resulting governing equation for φ in the hodograph plane can be solved with standard methods, since it is linear. [19] formulated a solution by means of eigenfunction expansion:

$$\varphi(\sigma, \lambda) = \sum_{k=1}^{\infty} J_0(2\alpha_k\sigma) \left[A_k \cos(\alpha_k\lambda) + B_k \sin(\alpha_k\lambda) \right], \tag{4}$$

with $\alpha_k = z_k/(2\sqrt{X_L})$, in which J_0 is the Bessel function of the first kind of order zero and z_k is its kth root. The solution in equation (4) implicitly incorporates the boundary conditions (2), while the yet unknown coefficients A_k and B_k are found after imposing the initial conditions (3). The dependent variables η and u in equations (1) are then found from equation (4), and the independent variables are calculated by inverting the hodograph transformation (i.e. $x = \sigma^2 - \eta$, $t = \lambda + u$), which resolves the wave field.

Since our purpose here is to compare run-up of different initial conditions rather than comparing their surface profiles and other properties, we skip further details of the solution and leave it to elsewhere [19,20]. The initial waves considered in this study are introduced in the next section.

2.2. Initial Wave Profiles and Their Shoreline Dynamics

The solitary wave profile is defined by [6] as

$$\eta_S(x) = H\operatorname{sech}^2(\gamma_S(x - x_c)), \quad \gamma_S = \sqrt{\frac{3H}{4}}, \tag{5}$$

where H is the initial wave amplitude, x_c is the center of the wave crest and γ_S is a wavenumber parameter defining the spread of the wave. We plot the solitary wave profile and the corresponding initial velocity distribution in the left-hand side panels of Figure 2. Respective temporal variations of the free surface height and the fluid velocity at the instantaneous shoreline tip ($x = X_S$) are plotted in the right-hand side panels.
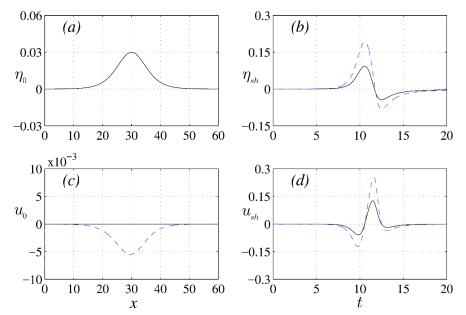

Figure 2. Shoreline dynamics for the solitary wave, equation (5). Panels (a) and (c) show the initial free surface elevation and the corresponding initial velocity distribution, respectively, for $H = 0.03$ and $x_c = 30$. Their temporal variations (η_{sh} and u_{sh}) at the moving shoreline tip ($x = X_S$) are presented in panels (b) and (d), respectively.

As a more realistic tsunami leading wave, [16] defined a family of N-waves. The first profile, called the *isosceles N-wave*, has the same elevation and depression heights and a constant separation distance. It is defined as

$$\eta_I(x) = \frac{3\sqrt{3}}{2} H \operatorname{sech}^2\big(\gamma_I(x - x_c)\big) \tanh\big(\gamma_I(x - x_c)\big), \quad \gamma_I = \frac{3}{2}\sqrt{H\sqrt{\frac{3}{4}}}. \tag{6}$$
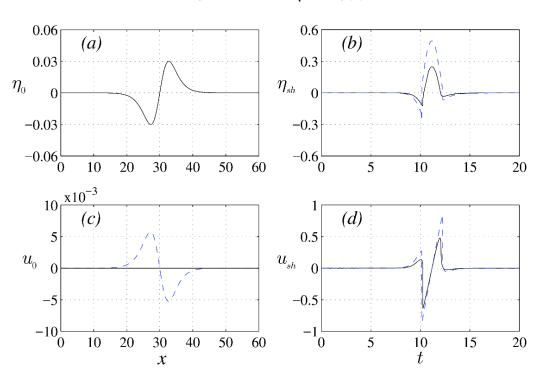
Another dipolar profile, again introduced by [16], but with different elevation and depression heights, is the *generalized N-wave* defined as

$$\eta_G(x) = \varepsilon H(x - x_2) \operatorname{sech}^2\big(\gamma_G(x - x_1)\big), \quad \gamma_G = \sqrt{\frac{3H}{4}}, \tag{7}$$

where x_1 and x_2 are two parameters controlling the locations of the wave crest and trough, and ε is a scaling parameter introduced to ensure the initial amplitude is H [16].

The N-wave profiles defined in equations (6) and (7) are plotted in Figures 3(a) and 4(a), with their corresponding initial velocity distributions in Figures 3(c) and 4(c). The time variations of the free surface height and wave velocity at the shoreline tip are presented in Figures 3(b,d) and 4(b,d), respectively.

The spatial distributions of the initial velocity of the wave profiles introduced above are calculated by using the exact non-linear relationship defined by [17] as

$$u_0(x) = 2\sqrt{x} - 2\sqrt{x + \eta_0(x)}. \tag{8}$$

Figure 3. Shoreline dynamics for the isosceles N-wave, equation (6). Panels (a) and (c) show the initial free surface elevation and the corresponding initial velocity distribution, respectively, for $H = 0.03$ and $x_c = 30$. Their temporal variations (η_{sh} and u_{sh}) at the shoreline tip ($x = X_S$) are presented in panels (b) and (d), respectively.
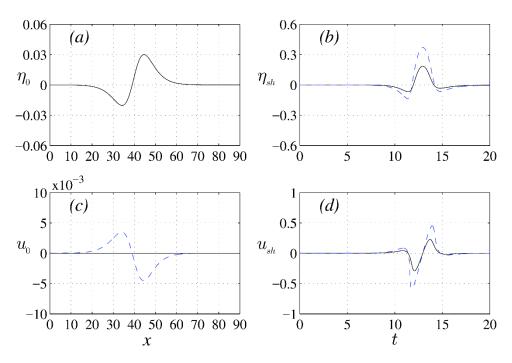
Figure 4. Shoreline dynamics for the generalized N-wave, equation (7). Panels (a) and (c) show the initial free surface elevation and the corresponding initial velocity distribution, respectively, for $H = 0.03$, $x_1 = 40$ and $x_2 = 39$, in which case the scaling parameter takes the value $\varepsilon = 0.278$ to ensure that the maximum initial wave amplitude is indeed 0.03. Temporal variations of the free surface elevation and the fluid velocity (η_{sh} and u_{sh}) at the shoreline tip ($x = X_S$) are presented in panels (b) and (d), respectively.

We should also note here that there are approximations to this equation; the linear approximation $u_0(x) \approx -\eta_0(x)/\sqrt{x}$ introduced by [21] and the asymptotic approximation $u_0(x) \approx -\eta_0(x)$ introduced by [22]. However, since the analytical method utilized here allows calculations with the exact equation, there is no need for an approximation. The initial wave velocities in the lower left panels of Figures 2 to 4 are calculated through equation (8).

In the next section we compare the run-up behavior of the initial wave types introduced above.

3. RESULTS AND DISCUSSION

Below we present results for solitary and N-wave tsunami initial conditions. We identify the maximum run-up behavior of these waves under non-zero initial velocity condition and compare our results with those belonging to the zero initial velocity case. We also demonstrate the effect of varying initial wave parameters such as amplitude or wave crest location on the maximum run-up. Such thorough comparison does not exist in the literature, except for the work by [17], who compares, for various initial wave locations, the maximum run-up of two different Gaussian-type initial wave profiles having identical amplitudes and the same initial velocity condition. Our examination here is more detailed as we compare the maximum run-ups of waves having different initial wave parameters and different initial velocity assumptions.

Wave run-up is defined as the free surface elevation at the shoreline tip (Figure 1), i.e.

$$R(t) = \eta(x = X_S, t), \qquad (9)$$

and the maximum run-up is defined to be its maximum value:

$$\boldsymbol{R} = \max_{t \geq 0} R(t). \tag{10}$$

[6] showed that the maximum run-up variation of the solitary wave defined in equation (5) with respect to the initial wave amplitude obeys the relation $\boldsymbol{R} \sim H^{5/4}$. [16] further demonstrated that the isosceles N-wave in equation (6) and the generalized N-wave in equation (7) follow exactly the same run-up law. These run-up behaviors are also confirmed by [23], although he formulated the problem as an initial value problem, unlike the boundary value problem approach of [6] and [16].

In Figure 5(a) solitary waves with different initial wave amplitudes (*H*) are plotted, while Figure 5(b) shows the maximum run-up variation of these waves. Similarly, Figure 5(c) shows solitary waves with different wave crest center values (x_c), and Figure 5(d) shows the maximum run-up variation for these parameters. In order to exhibit the asymptotic behavior of the maximum run-up variations and compare with the existing solutions in the literature, the right-hand side panels (b) and (d) of Figure 5 are plotted using the logarithmic scale.

Similar results are presented for the isosceles N-wave in Figure 6, and for the generalized N-wave in Figure 7. We remark here that, for the generalized N-wave case, the maximum run-up variation is only plotted for varying *H* in Figure 7(b); since there are two parameters (x_1 and x_2) involved in the generalized N-wave formula, standing for the elevation and depression locations, and since changing one of these parameters moves locations of both the crest and the trough of the initial wave, we did not include the case of varying x_1 and x_2 in our analysis here.
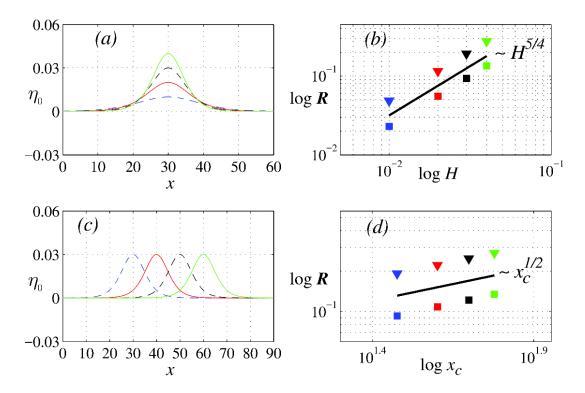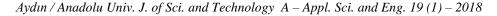

Figure 5. Maximum run-up variation of the solitary wave. The initial wave amplitude *H* of the solitary wave is varied from 0.01 to 0.04 with 0.01 increment in panel (a), while the wave crest location is fixed to $x_c = 30$, and x_c is varied from 30 to 60 with 10 increment in panel (c), while the amplitude is fixed to $H = 0.03$. The respective maximum run-up variations are plotted in panels (b) and (d) for zero (squares) and non-zero (triangles) initial velocity conditions, using the logarithmic scale.
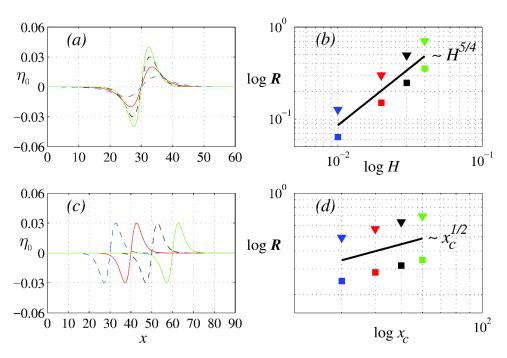
Figure 6. Maximum run-up variation of the isosceles N-wave. The initial wave amplitude H is varied from 0.01 to 0.04 with 0.01 increment in panel (a), while the wave crest is fixed to $x_c = 30$, and the center location x_c is varied from 30 to 60 with 10 increment in panel (c), while the amplitude is fixed to $H = 0.03$. The respective maximum run-up variations are plotted in panels (b) and (d) for zero (squares) and non-zero (triangles) initial velocity conditions, using the logarithmic scale.
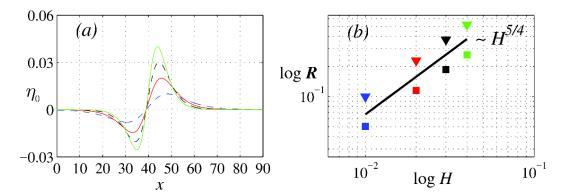

Figure 7. Maximum run-up variation of the generalized N-wave. The initial wave amplitude H is varied from 0.01 to 0.04 with 0.01 increment in panel (a), while $x_1 = 40$ and $x_2 = 39$ are fixed. The corresponding maximum run-up variation is plotted in panel (b) for zero (squares) and non-zero (triangles) initial velocity, using the logarithmic scale.

The results presented in Figures 5 to 7 reveal that the maximum run-up variation with respect to the initial wave amplitude H in the presence of initial fluid velocity is exactly the same as that of the zero-velocity case. In other words, existence of initial velocity does not change the maximum run-up behavior; under both zero and non-zero initial velocity conditions, the maximum run-up of solitary, isosceles, and generalized N-waves obey the same asymptotic relation, namely $R \sim H^{5/4}$.

In this study we also obtained the maximum run-up variation for solitary and isosceles N-waves with respect to the wave crest location x_c. Our analysis manifests that the maximum tsunami run-up changes with the square root of the wave crest location, i.e. $R \sim x_c^{1/2} = \sqrt{x_c}$. Moreover, this tendency remains valid in the presence of initial velocity, just as in the case for amplitude.

Finally, the numerical values of the maximum wave run-up for solitary wave and isosceles and generalized N-waves with and without initial velocity are presented in the table below. It is apparent that existence of initial velocity almost doubles the free surface height calculated at the shoreline.

Table. The maximum run-up values calculated for the solitary wave, the isosceles N-wave and the generalized N-wave introduced in equations (5)-(7). The third column includes values for the zero velocity case ($u_0 \equiv 0$), while the last column employs run-up values under non-zero initial fluid velocity condition ($u_0 \neq 0$), calculated from equation (8).

Initial wave type	Parameters	Maximum run-up (R)	
		$u_0(x) \equiv 0$	$u_0(x) \neq 0$
Solitary wave, equation (5)	$H = 0.03, x_c = 30$	0.0930	0.1916
Isosceles N-wave, equation (6)	$H = 0.03, x_c = 30$	0.2480	0.4939
Generalized N-wave, equation (7)	$H = 0.03; x_1 = 40, x_2 = 39$	0.1829	0.3658

4. CONCLUSIONS

In this study we attempted to obtain the maximum tsunami run-up resulting from solitary and N-wave initial conditions in the presence of initial velocity, which simulates submarine landslide tsunamis or tectonic tsunamis with low rupture speed. For this purpose, the non-linear shallow-water wave equations are solved analytically as an initial-boundary value problem, using the separation of variables technique. This solution strategy can handle the general problem of realistic surface profiles having initial velocity. Besides, it is a fast and accurate method, unlike integral transform techniques.

The maximum run-up values are obtained analytically for solitary and N-waves with non-zero velocity profiles, and the results are compared with the zero-velocity case. The non-zero initial velocity distribution is calculated by using the exact non-linear initial fluid velocity relation, without needing any further simplifications, thanks to the solution method utilized. The results suggest that the maximum run-up produced by initial waves starting with non-zero velocity is increased significantly, reaching twice the run-up of waves without initial velocity. On the other hand, it is observed that the presence of non-zero fluid velocity does not change the run-up behavior. That is, waves with initial velocity exhibit the same asymptotic run-up variation as waves without initial velocity, for all initial wave types considered here. This trend is observed both for varying initial amplitude and also varying wave crest location. To the author's best knowledge, the latter case is examined for the first time in this study.

ACKNOWLEDGEMENTS

REFERENCES

[1] Gusiakov VK. Tsunami History: Recorded. In: Bernard EN, Robinson AR, editors. The Sea, Volume 15: Tsunamis. Cambridge, MA, USA and London, England: Harvard University Press, 2009. pp. 23-53.

[2] Intergovernmental Oceanographic Commission. Tsunami Glossary, 2008. Paris, UNESCO: IOC Technical Series, 85, 2008.

[3] Carrier GF, Greenspan HP. Water waves of finite amplitude on a sloping beach. J Fluid Mech 1958; 4: 97-109.

[4] Keller JB, Keller HB. Water wave run-up on a beach. ONR Research Report NONR-3828(00), Department of the Navy, Washington, DC, USA, 1964.

[5]   Peregrine DH. Long waves on a beach. J Fluid Mech 1967; 27: 815-827.

[6]   Synolakis CE. The runup of solitary waves. J Fluid Mech 1987; 185: 523-545.

[7]   Hibbert SD, Peregrine H. Surf and runup on a beach: a uniform bore. J Fluid Mech 1979; 95: 323-345.

[8]   Pedersen G, Gjevik B. Run-up of solitary waves. J Fluid Mech 1983; 135: 283-299.

[9]   Zelt JA. The run-up of nonbreaking and breaking solitary waves. Coast Eng 1991; 15: 205-246.

[10] Li Y, Raichlen F. Non-breaking and breaking solitary wave run-up. J Fluid Mech 2002; 456: 295-318.

[11] Kim SK, Liu PLF, Liggett JA. Boundary integral equation solutions for solitary wave generation, propagation and run-up. Coast Eng 1983; 7: 299-317.

[12] Hall JV, Watts, JW. Laboratory investigation of the vertical rise of solitary waves on impermeable slopes. Tech. Memo. 33, Beach Erosion Board, USACE, 1953.

[13] Street RL, Camfield FE. Observations and experiments on solitary wave deformation. In: Tenth International Conference on Coastal Engineering; September 1966; Tokyo, Japan: ASCE. pp. 284-301.

[14] Hammack JL. A note on tsunamis: their generation and propagation in an ocean of uniform depth. J Fluid Mech 1973; 60: 769-799.

[15] Synolakis CE, Bernard EN. Tsunami science before and beyond Boxing Day 2004. Phil Trans R Soc A 2006; 364: 2231-2265.

[16] Tadepalli S, Synolakis CE. The run-up of N-waves on sloping beaches. Proc R Soc London A 1994; 445: 99-112.

[17] Kânoğlu U, Synolakis CE. Initial value problem solution of nonlinear shallow water-wave equations. Phys Rev Lett 2006; 148501.

[18] Stoker JJ. Water Waves: The Mathematical Theory with Applications. Wiley Classics Library ed. New York, NY, USA: John Wiley & Sons, Inc., 1992.

[19] Aydın B. Analytical solutions of shallow-water wave equations. PhD, Middle East Technical University, Ankara, Turkey, 2011.

[20] Aydın B, Kânoğlu U. New analytical solution for nonlinear shallow water-wave equations. Pure Appl Geophys 2017; 174: 3209-3218.

[21] Carrier GF, Wu TT, Yeh H. Tsunami run-up and draw-down on a plane beach. J Fluid Mech 2003; 475: 79-99.

[22] Prichard D, Dickinson L. The near-shore behaviour of shallow-water waves with localized initial conditions. J Fluid Mech 2007, 591: 413-436.

[23] Kânoğlu U. Nonlinear evolution and runup-rundown of long waves over a sloping beach. J Fluid Mech 2004; 513: 363-372.